Global climate evolution during the last deglaciation

Peter U. Clark[a,1], Jeremy D. Shakun[b,1], Paul A. Baker[c], Patrick J. Bartlein[d], Simon Brewer[e], Ed Brook[a], Anders E. Carlson[f,g], Hai Cheng[h,i], Darrell S. Kaufman[j], Zhengyu Liu[g,k], Thomas M. Marchitto[l], Alan C. Mix[a], Carrie Morrill[m], Bette L. Otto-Bliesner[n], Katharina Pahnke[o], James M. Russell[p], Cathy Whitlock[q], Jess F. Adkins[r], Jessica L. Blois[g,s], Jorie Clark[a], Steven M. Colman[t], William B. Curry[u], Ben P. Flower[v], Feng He[g], Thomas C. Johnson[t], Jean Lynch-Stieglitz[w], Vera Markgraf[j], Jerry McManus[x], Jerry X. Mitrovica[b], Patricio I. Moreno[y], and John W. Williams[s]

[a]College of Earth, Ocean, and Atmospheric Sciences, Oregon State University, Corvallis, OR 97331; [b]Department of Earth and Planetary Sciences, Harvard University, Cambridge, MA 02138; [c]Division of Earth and Ocean Sciences, Duke University, Durham, NC 27708; [d]Department of Geography, University of Oregon, Eugene, OR 97403; [e]Department of Geography, University of Utah, Salt Lake City, UT 84112; [f]Department of Geoscience, University of Wisconsin, Madison, WI 53706; [g]Center for Climatic Research, University of Wisconsin, Madison, WI 53706; [h]Institute of Global Environmental Change, Xi'an Jiaotong University, Xi'an 710049, China; [i]Department of Geology and Geophysics, University of Minnesota, Minneapolis, MN 55455; [j]School of Earth Sciences and Environmental Sustainability, Northern Arizona University, Flagstaff, AZ 86011; [k]Laboratory for Ocean-Atmosphere Studies, School of Physics, Peking University, Beijing 100871, China; [l]Institute of Arctic and Alpine Research, University of Colorado, Boulder, CO 80309; [m]National Oceanic and Atmospheric Administration National Climatic Data Center, Boulder, CO 80305; [n]Climate and Global Dynamics Division, National Center for Atmospheric Research, Boulder, CO 80307; [o]Department of Geology and Geophysics, University of Hawaii, Honolulu, HI 96822; [p]Department of Geological Sciences, Brown University, Providence, RI 02912; [q]Department of Earth Sciences, Montana State University, Bozeman, MT 97403; [r]Division of Geological and Planetary Sciences, California Institute of Technology, Pasadena, CA 91125; [s]Department of Geography, University of Wisconsin, Madison, WI 53706; [t]Large Lakes Observatory and Department Geological Sciences, University of Minnesota, Duluth, MN 55812; [u]Department of Geology and Geophysics, Woods Hole Oceanographic Institution, Woods Hole, MA 02543; [v]College of Marine Science, University of South Florida, St. Petersburg, FL 33701; [w]School of Earth and Atmospheric Sciences, Georgia Institute of Technology, Atlanta, GA 30332; [x]Lamont-Doherty Earth Observatory, Palisades, NY 10964; and [y]Institute of Ecology and Biodiversity and Department of Ecological Sciences, Universidad de Chile, Santiago 1058, Chile

AUTHOR SUMMARY

Deciphering the evolution of global climate from the end of the Last Glacial Maximum (LGM) approximately 19 ka to the early Holocene 11 ka presents an outstanding opportunity for understanding the transient response of Earth's climate system to external and internal forcings. During this interval of global warming, virtually every component of the climate system underwent large-scale change, sometimes at extraordinary rates, as the world emerged from the grips of the last ice age. This dramatic time of global change was triggered by changes in insolation, with associated changes in ice sheets, greenhouse gas concentrations, and other amplifying feedbacks that produced distinctive regional and global responses. In addition, there were several episodes of large and rapid sea-level rise and abrupt climate change that produced regional climate signals superposed on those associated with global warming. Considerable ice-sheet melting and sea-level rise occurred after 11 ka, but otherwise the world had entered the current interglaciation with near-pre-Industrial greenhouse gas concentrations and relatively stable climates. Here we summarize a major effort by the paleoclimate research community to characterize these changes through the development of well-dated, high-resolution records of the deep and intermediate ocean as well as surface climate.

Several proxies identify large changes in the volume and circulation of the major water masses that fill the deep ocean. During the LGM, there was a marked division in the Atlantic, Indian, and Pacific oceans separating shallower,

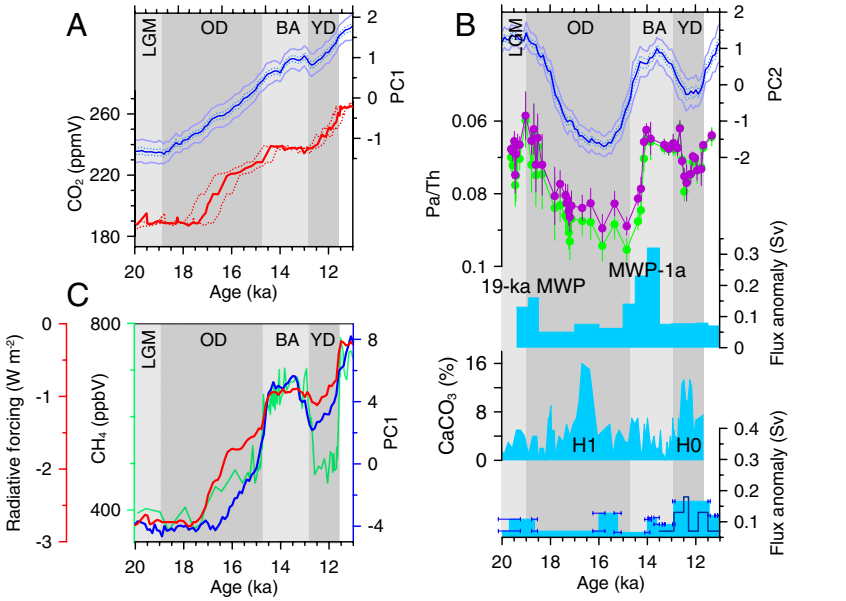

Fig. P1. (*A*) Comparison of the global temperature PC1 (blue line, with confidence intervals showing results of jackknifing procedure for 68% and 95% of records removed) with record of atmospheric CO_2 from European Project for Ice Coring in Antarctica Dome C ice core (red line with age uncertainty) (4) on revised timescale from ref. 5. (*B*) Comparison of the global temperature PC2 (blue line, with confidence intervals showing results of jackknifing procedure for 68% and 95% of records removed) with Pa/Th record (a proxy for Atlantic meridional overturning circulation) (3) (green and purple symbols). Also shown are freshwater fluxes from ice-sheet meltwater, Heinrich events, and routing events. (*C*) Comparison of the global precipitation PC1 (blue line) with record of methane (green line) and radiative forcing from greenhouse gases (red line). OD, Oldest Dryas; BA, Bølling—Allerød; YD, Younger Dryas; MWP, meltwater pulse.

Author contributions: P.U.C., J.D.S., Z.L., and B.L.O.-B. designed research; P.U.C., J.D.S., and J.X.M. performed research; P.U.C., J.D.S., A.E.C., H.C., Z.L., B.L.O.-B., J.F.A., J.L.B., J.C., S.M.C., W.B.C., B.P.F., F.H., T.C.J., J.L.-S., V.M., J.M., P.I.M., and J.W.W. analyzed data; and P.U.C., J.D.S., P.A.B., P.J.B., S.B., E.B., A.E.C., D.S.K., T.M.M., A.C.M., C.M., K.P., J.M.R., and C.W. wrote the paper.

The authors declare no conflict of interest.

This article is a PNAS Direct Submission.

[1]To whom correspondence may be addressed. E-mail: clarkp@onid.orst.edu or shakun@fas.harvard.edu.

See full research article on page E1134 of www.pnas.org.

Cite this Author Summary as: PNAS 10.1073/pnas.1116619109.

nutrient-poor intermediate water from more nutrient-rich deep water. In the North Atlantic, Antarctic Bottom Water expanded northward and upward at the expense of North Atlantic Deep Water (NADW), while both water masses maintained a vigorous circulation. In the southwest Pacific and the Arabian Sea, there was an increased influence of Antarctic Intermediate Water (AAIW). During the subsequent deglaciation, there was a net decrease of the Atlantic meridional overturning circulation (AMOC) below LGM strength during the Oldest Dryas, renewed production of NADW at the start of the Bølling–Allerød, followed by a subsequent decrease during the Younger Dryas. In the southwest Pacific and the Arabian Sea, the influence of AAIW further increased during the Oldest Dryas, decreased again during the Bølling–Allerød, and subsequently increased during the Younger Dryas. In contrast, intermediate-depth sites in the southeast Pacific suggest greatest expansion of AAIW during the LGM, followed by stepwise reduction between 17 and 11 ka.

The low concentrations of atmospheric CO_2 during the LGM are thought to have been caused by greater storage of carbon in the deep ocean through stratification of the Southern Ocean (1). Release of the sequestered carbon may have occurred due to deep Southern Ocean overturning induced by enhanced wind-driven upwelling and sea-ice retreat associated with times of Antarctic warming, coincident with the Oldest and Younger Dryas cold events in the north.

We used empirical orthogonal functions (EOFs) to provide an objective characterization of the temporal and spatial patterns of the leading modes of global surface climate variability for the 20- to 11-ka interval as derived from 166 published proxy records. In addition to characterizing sea surface temperature (SST) variability, we also characterize variability in regional and global continental temperature and precipitation, as well as derive a composite of global temperature variability.

Our analysis indicates that the superposition of two orthogonal modes explains much of the variability (64–100%) in regional and global climate during the last deglaciation (Fig. P1). The nearly uniform spatial pattern of the global temperature EOF1 and the large magnitude of the temperature principal component 1 (PC1) variance indicate that this mode reflects the global warming of the last deglaciation. Given the large global forcing of greenhouse gases (GHGs) (2), the strong correlation between PC1 and the combined GHG forcing ($r^2 = 0.97$) (Fig. P1) supports arguments that GHGs were a major driver of global warming.

In contrast, the global temperature PC2 is remarkably similar to a North Atlantic Pa/Th record ($r^2 = 0.86$) (Fig. P1) that is interpreted as a kinematic proxy for the strength of the AMOC (3). Similar millennial-scale variability is identified in several other proxies of intermediate- and deep-ocean circulation, identifying a strong coupling between SSTs and ocean circulation. The large reduction in the AMOC during the Oldest Dryas can be explained as a response to the freshwater forcing associated with the 19-ka meltwater pulse from Northern Hemisphere ice sheets, Heinrich event 1, and routing events along the southern Laurentide Ice Sheet margin, whereas the reduction during the Younger Dryas was likely caused by freshwater routing through the St. Lawrence River and Heinrich event 0. The sustained strength of the AMOC following meltwater pulse 1a supports arguments for a large contribution of this event from Antarctica . With EOF2 accounting for only 13% of deglacial global climate variability, we conclude that the direct global impact of AMOC variations was small in comparison to other processes operating during the last deglaciation.

The global precipitation EOF1 shows a more complex spatial response than the global temperature EOF1, whereas the initial increase in the associated PC1 significantly lags the initial increase in the global temperature PC1 and exhibits greater millennial-scale structure than seen in the global temperature PC1 (Fig. P1). Insofar as precipitation increases should accompany a warming planet, the approximately 2-ky lag between the initial increase in temperature and precipitation may reflect one or more mechanisms that affect low-latitude hydrology, including the impact of Oldest Dryas cooling, a nonlinear response to Northern Hemisphere forcing by insolation and glacial boundary conditions, or interhemispheric latent heat transports. This response may then have been modulated by subsequent millennial-scale changes in the AMOC and its attendant effects on African and Asian monsoon systems and the position of the Intertropical Convergence Zone and North American storm tracks.

1. Toggweiler JR (1999) Variation of atmospheric CO_2 by ventilation of the ocean's deepest water. *Paleoceanography* 14:571–588.
2. Broccoli AJ (2000) Tropical cooling at the Last Glacial Maximum: An atmosphere-mixed layer ocean model simulation. *J Climate* 13:951–976.
3. McManus JF, Francois R, Gherardi JM, Keigwin LD, Brown-Leger S (2004) Collapse and rapid resumption of Atlantic meridional circulation linked to deglacial climate changes. *Nature* 428:834–837.
4. Monnin E, et al. (2001) Atmospheric CO_2 concentrations over the last glacial termination. *Science* 291:112–114.
5. Lemieux-Dudon B, et al. (2010) Consistent dating for Antarctic and Greenland ice cores. *Quat Sci Rev* 29:8–20.